

**High- $p_T$  resonances as a possibility to explore hot and dense nuclear matter**S. Vogel,<sup>1,2</sup> J. Aichelin,<sup>2</sup> and M. Bleicher<sup>1</sup><sup>1</sup>*Institut für Theoretische Physik, J. W. Goethe Universität, Max-von-Laue-Straße 1, D-60438 Frankfurt am Main, Germany*<sup>2</sup>*SUBATECH, Laboratoire de Physique Subatomique et des Technologies Associées, University of Nantes-IN2P3/CNRS-Ecole des Mines de Nantes, 4 rue Alfred Kastler, F-44072 Nantes Cedex 03, France*

(Received 31 August 2009; published 29 July 2010)

One of the fundamental objectives of experiments with ultrarelativistic heavy ions is to explore strongly interacting matter at high baryon density and high temperature. In this investigation we apply a hadronic transport approach to study in particular the information that can be obtained by analyzing baryonic and mesonic resonances. The decay products of these resonances carry information on the resonances properties at the space-time point of their decay. We especially investigate the percentage of reconstructable resonances as a function of baryon density for heavy-ion collisions in the energy range between  $E_{\text{lab}} = 30$  A GeV and  $\sqrt{s} = 200$  A GeV, the energy domain between the future GSI Facility for Antiproton and Ion Research and the present BNL Relativistic Heavy Ion Collider. It is shown that a transverse-momentum-dependent analysis of resonances might be beneficial for investigating the high-baryon-density phase of heavy-ion collisions.

DOI: [10.1103/PhysRevC.82.014907](https://doi.org/10.1103/PhysRevC.82.014907)

PACS number(s): 24.10.Lx, 25.75.Dw, 21.65.-f

**I. INTRODUCTION**

The experimental analysis of heavy-ion reactions using resonances has been applied for several years from low-energy [1,2], through intermediate-energy [3,4], to high-energy heavy-ion collisions [5–7]. In general, one distinguishes between leptonic and hadronic decay channels. While the hadronic decay channels have the advantage of larger branching ratios, the leptonic decays have the advantage that the decay particles do not undergo final state interactions. Thus, it is worthwhile to work out the differences and the advantages and disadvantages of the two approaches that are discussed in the following.

The present Relativistic Heavy Ion Collider (RHIC) at Brookhaven and the upcoming GSI Facility for Antiproton and Ion Research (FAIR; for a recent overview on the status of the project, we refer the reader to Ref. [8]) provide an excellent research environment for probing resonances in matter. In the RHIC experiments it has been observed [9] that less resonances are measured than expected from statistical model calculations [10]. Stable hadrons, however, follow the prediction of this model. This suggests the conclusion that after chemical freeze-out, when the chemical composition of the final state is determined, hadrons still undergo collisions and therefore some of the resonances cannot be identified by the invariant mass of the decay products.

At FAIR the leptonic and the hadronic decay channels can be explored. While the leptonic channel is usually regarded as the “cleaner” channel, recent calculations [11] have shown that the dilepton channel might not probe the dense phase as was expected before.

In light of this new development, it is worthwhile to evaluate the density-profile and the space-time evolution of resonances that can be reconstructed in the hadronic decay channels. Although those channels suffer from the drawback of final-state interaction of the decay products, their large branching ratios might make them better suited for the investigation of the high-density phase of heavy-ion collisions compared to leptonic decay channels.

**II. MODEL DESCRIPTION**

For our calculations we utilize the UrQMD(v2.3) model, a nonequilibrium transport approach that relies on the covariant Boltzmann equation. All cross sections are calculated by the principle of detailed balance and the additive quark model or are fitted to available experimental data. UrQMD does not include any explicit in-medium modifications for vector mesons or effects to describe the restoration of chiral symmetry.

Resonances interact with all other particles given that the collision criterion is met [ $d < \sqrt{\sigma/\pi}$ , with  $d$  being the distance of closest approach and  $\sigma$  being the cross section of the binary collision]. Thus, reabsorption and collisional broadening is dynamically implemented. The resonance parameters (pole masses and total and partial decay widths at the pole) are within the limits of Ref. [12].

The model makes it possible to study the full space-time evolution of all hadrons, resonances, and their decay products in hadron-hadron or nucleus-nucleus collisions. This makes it possible to explore the emission patterns of resonances in detail and to gain insight into their origins and decay channels. For previous studies of resonances within this model, see Refs. [11,13–18].

For further details about the UrQMD model, the reader is referred to Refs. [19,20].

Experimentally, the reconstruction of resonances is challenging. One often-applied technique is to reconstruct the invariant mass spectrum for single events. Then an invariant mass distribution of mixed events is generated (here the particle pairs are uncorrelated by definition). The mixed event distribution is subtracted from the invariant mass spectrum of the single (correlated) events. As a result, one obtains the mass distributions and yields (after all experimental corrections) of the resonances by fitting the resulting distribution with a suitable function (usually a Breit-Wigner function peaked around the pole mass of the respective resonance).

If the resonance spectral function changes in the hadronic medium, this is in principle visible in the difference spectrum between true and mixed events. However, if a daughter particle

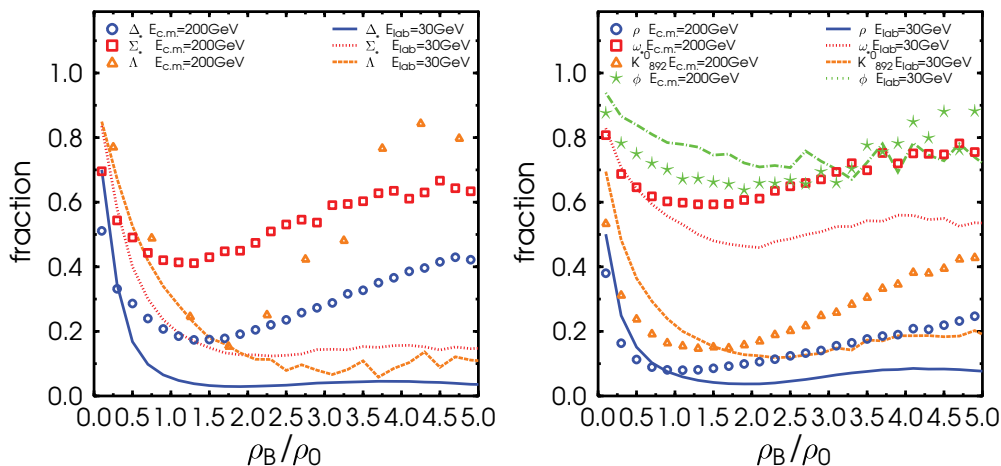


FIG. 1. (Color online) Fraction of reconstructable baryon resonances (left) and meson resonances (right) as a function of baryon density at the point of production.

(re-)scatters before reaching the detector, the signal for the experimental reconstruction is blurred or even lost. Especially for strongly interacting decay products, this effect can be sizable. It is therefore difficult to judge whether a deviation from an expected Breit-Wigner distribution is attributable to an initial deformation or an increase of the initial width or to the momentum dependence of the rescattering cross section of the daughter particles.

What makes this analysis even tougher is the fact that the resonances decay over a wide range of densities and therefore only an average value is measured. If this average value is dominated by resonance decays at low density the information from the high-density phase is blurred and may offer only a limited view on the high-density phase of the heavy-ion collision.

In the UrQMD model we apply a different technique for the extraction of resonances. This method makes it possible to trace all resonances that are, in principle, reconstructable. We follow the individual decay products of each decaying resonance (the daughter particles). If the daughter particles do not rescatter in the further evolution of the system, the resonance is counted as “reconstructable.” The advantage of this method is that it makes it possible to trace back the origin of each individual resonance to study their spatial and temporal emission pattern. Because UrQMD follows the space-time evolution of all particles, it is possible to link the production and decay points of each individual resonance. This method also makes it possible to explore the reconstruction efficiency in different decay branches. Note, however, that this method is restricted to theoretical models and not applicable in experimental analyses.

To calculate at which density the resonance decays, we have to determine the baryonic density. The baryon density is calculated locally at the position of the resonance in the rest frame of the baryon current (Eckart frame) as  $\rho_B = j^0$  with  $j^\mu = (\rho_B, \vec{0})$ . Details on the calculation of the baryon density are discussed in Ref. [11]. One should note that the method chosen is insensitive to the parameters of the density calculation if chosen within reasonable bounds. A variation of the Gaussian widths by 50% resulted in no difference in the

obtained results. All densities mentioned in the text and figures are baryon densities. In all figures we present the density in units of nuclear ground-state density  $\rho_0$ , where a value of  $0.16 \text{ fm}^{-3}$  is assumed. We chose the density at the point of production to have a handle on the maximum of the expected effect. However, one should note that the spectral function of a resonance is sensitive to the properties of the medium it experiences during its evolution between production and decay (or absorption). In the following we discuss the density dependence of the probability that a resonance can be reconstructed. Naively, one would expect that the higher the densities the more the rescattering effect becomes dominant. Therefore, it is unlikely that a resonance that decays at high density is reconstructable. The view on the low-density zone is expected to remain unblurred but is less interesting because it resembles that observed in elementary collisions.

All analyses presented in this work are done for central (impact parameter  $b \leq 3.4 \text{ fm}$ ) Au + Au collisions at either FAIR energies of  $E_{\text{lab}} = 30 \text{ A GeV}$  or top RHIC energies of  $\sqrt{s} = 200 \text{ A GeV}$ .

### III. RESONANCES AT HIGH TRANSVERSE MOMENTUM

The left (right) panel of Fig. 1 shows the probability that a baryon resonance—shown are  $\Delta$ ,  $\Sigma^*(1385)$ , and  $\Lambda^*(1520)$  baryon resonances ( $\rho$ ,  $\omega$ ,  $K^{*0}$ , and  $\phi$  mesons)—which was produced at a certain density can be reconstructed experimentally. One observes a clear peak at very low density and a steady decrease toward higher density. This means that resonances that are produced at rather low density have a high probability of being detected and as the density increases the chance of reconstructing the resonances decreases. This is nothing unexpected. However, this trend stops at roughly  $2 \rho_0$ . At higher densities the chance of reconstructing a resonance stabilizes or even increases slightly again. This increase, which we discuss later in detail, is caused by resonances which picked up very high transverse momenta and leave the interaction zone quickly. This results in a decay in a region with less hadronic activity and a higher chance of being reconstructed.

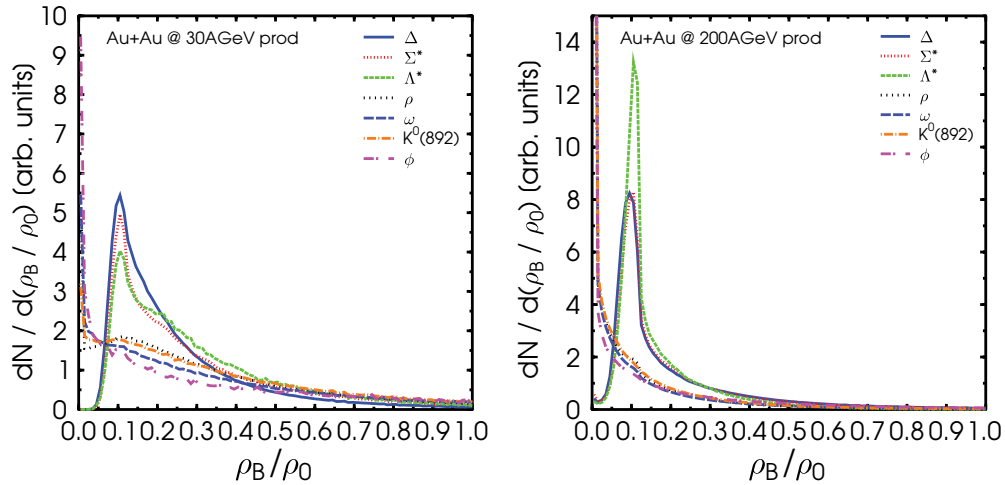


FIG. 2. (Color online) Probability distribution of baryon density at the production vertex for various reconstructable resonances in central ( $b \leq 3.4$  fm) Au + Au collisions at 30 A GeV (left panel) and 200 A GeV (right panel) as a function of baryon density. One observes that most resonances that can be reconstructed in the hadronic decay channel originate from low baryon density.

Whereas the form of the curves is qualitatively similar for the different hadrons the absolute value of the fraction of reconstructable resonances is rather different. It can be understood in terms of lifetimes of the resonances and in terms of the rescattering cross sections of the decay products.

Owing to the large cross section of pions in nuclear matter (usually undergoing  $N + \pi \rightarrow \Delta$  or  $\pi + \pi \rightarrow \rho$  reactions) the probability of detecting a high-density  $\Delta$  resonance or a  $\rho$  meson is rather small compared to the probability of detecting a high-density  $\phi$  meson, since the  $\phi$  meson itself has a small cross section in nuclear matter and a long lifetime of  $\sim 40$  fm/c and the hadronic decay products (mostly kaons and antikaons) have a smaller cross sections when compared to the pions from the decay of a  $\rho$  meson. Similarly, the long lifetime of the  $\Lambda$  increases their possibility of being reconstructed. As mentioned earlier, the saturation or slight increase of the reconstruction probability as a function of density has its origin in the possibility that resonances with a large  $p_T$  can escape quickly from the reaction zone, which is rather small initially.

Figure 2 shows for various resonances the probability that an experimentally reconstructable resonance has been created at a density  $\rho_B$ . The integral over all densities is normalized to unity. One observes that most of those resonances are produced at very low densities, which is especially true for the mesonic resonances.

Reconstructable baryon resonances stem from slightly higher baryon densities; however, most are still produced at rather low densities (with a peak at roughly 0.1 ground-state density). So the detection of resonances produced at densities above ground-state densities using hadronic decay channels seems not too encouraging. However, as we discuss next, an alternative method of circumventing that problem might exist.

Let us illustrate this further with two examples (one baryon, one meson) that are representative for all investigated particles.

Figure 3 depicts the average transverse momentum of  $\Delta$ -baryon and  $\rho$ -meson resonances as a function of baryon density. Lines show reconstructable resonances; symbols show

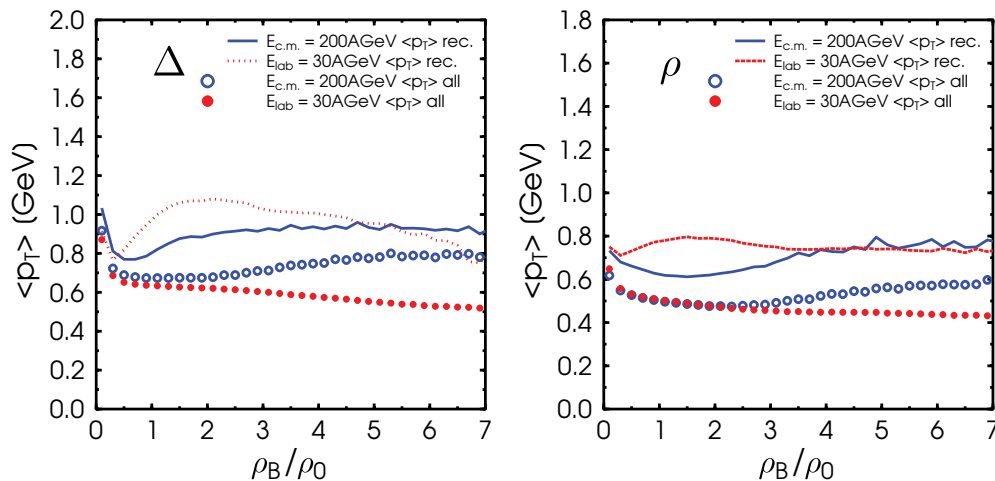


FIG. 3. (Color online) Average transverse momentum of reconstructable (lines) or all (symbols)  $\Delta$  baryons (left panel) and  $\rho$  mesons (right panel) as a function of baryon density for two different energies.

all decayed resonances. The striking feature is the different average transverse momentum between all resonances and those that are reconstructable. The higher the average transverse momentum, the larger is the chance that the resonance can be reconstructed. The  $\langle p_T \rangle$  of reconstructable  $\Delta/\rho$  resonances is about 200 MeV higher than for all  $\Delta/\rho$  resonances. Resonances with a large  $p_T$  can leave the high-density zone rather fast and move with a velocity of about  $\langle p_T \rangle/E$  outward.

Another interesting feature in Fig. 3 is the difference between the  $\sqrt{s} = 200$  A GeV and  $E_{\text{lab}} = 30$  A GeV curves. While the  $E_{\text{lab}} = 30$  A GeV data show a decrease of  $\langle p_T \rangle$  as a function of the baryon density, the  $\sqrt{s} = 200$  A GeV data show an increase. At  $\sqrt{s} = 200$  A GeV the initial collisions (which happen at high baryon density) are more energetic and give the particles a high transverse momentum, and subsequent scattering decreases  $p_T$ . For the  $E_{\text{lab}} = 30$  A GeV collisions the situation is opposite. Initially, the particle  $p_T$  is small and the interaction with the medium increases the  $p_T$  due to transverse expansion.

Figure 4 shows the  $p_T$  dependence of the reconstruction probability in detail. It shows the transverse momentum spectra for all (full symbols) and reconstructable resonances (open symbols). The numbers stated in the three shaded areas ( $p_T < 1$  GeV,  $1 \text{ GeV} < p_T < 2$  GeV,  $p_T > 2$  GeV) are the percentages of reconstructable resonances created at a density higher than  $2\rho_0$ . One observes that at low transverse momentum the percentage of reconstructable resonances is low and increases when going to higher transverse momenta; that is, with increasing  $p_T$  the chance of reconstructing a resonance produced at high baryon density increases.

#### IV. CONCLUSIONS

In conclusion, we have discussed that the view on the high-density zone may not be as restricted as usually assumed when analyzing hadronic resonances.

We argued that resonances detected with high transverse momentum are sensitive to higher densities. It will be interesting to explore if the production properties of these

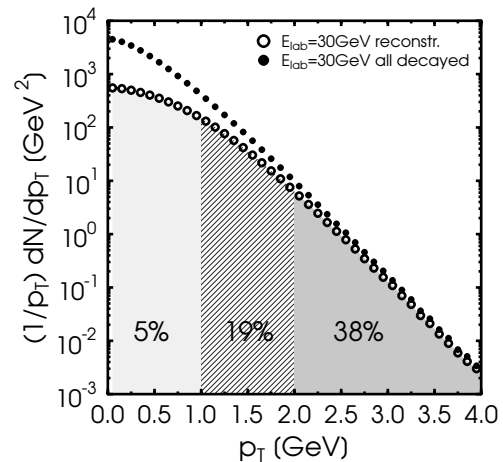


FIG. 4. Transverse momentum spectra for all and reconstructable resonances for central ( $b \leq 3.4$  fm) Au + Au collision at 30 A GeV beam energy. Solid circles depict the spectrum for all decayed resonances (included in the analysis are  $\Delta$ ,  $\Lambda$ , and  $\Sigma$  baryons, as well as  $\rho$ ,  $\omega$ ,  $K^{*0}$ , and  $\phi$  mesons); open circles depict the reconstructable resonances. The numbers indicate the percentage of reconstructable resonances stemming from the density region with  $\rho_B/\rho_0 > 2$ .

resonances are different from the bulk emitted at low densities. The exploration of high- $p_T$  resonances might therefore open a new keyhole in the upcoming Compressed Baryonic Matter (CBM) experiment at FAIR or the critRHIC program to gain information on the high-density zone and to observe eventual changes of resonance properties in the medium.

This work was financially supported by the Helmholtz International Center for FAIR within the framework of the LOEWE program (Landesoffensive zur Entwicklung Wissenschaftlich-Ökonomischer Exzellenz) launched by the State of Hesse. The computational resources have been provided by the Center for the Scientific Computing at Frankfurt. This work was supported by GSI, DAAD (PROCOPE), and BMBF.

- 
- [1] G. Agakichiev *et al.* (HADES Collaboration), *Phys. Rev. Lett.* **98**, 052302 (2007).
  - [2] X. Lopez *et al.*, *Phys. Rev. C* **76**, 052203 (2007).
  - [3] S. V. Afanasev *et al.* (NA49 Collaboration), *J. Phys. G* **27**, 367 (2001).
  - [4] D. Adamova *et al.* (CERES Collaboration), *Phys. Rev. Lett.* **91**, 042301 (2003).
  - [5] J. Adams *et al.* (STAR Collaboration), *Phys. Rev. Lett.* **97**, 132301 (2006).
  - [6] B. I. Abelev *et al.* (STAR Collaboration), *Phys. Rev. C* **78**, 044906 (2008).
  - [7] P. Fachine, *J. Phys. G* **35**, 044032 (2008).
  - [8] W. F. Henning, *Nucl. Phys. A* **805**, 502 (2008).
  - [9] C. Markert (STAR Collaboration), *J. Phys. G* **35**, 044029 (2008).
  - [10] A. Andronic, P. Braun-Munzinger, K. Redlich, and J. Stachel, *Nucl. Phys. A* **715**, 529 (2003).
  - [11] S. Vogel, H. Petersen, K. Schmidt, E. Santini, C. Sturm, J. Aichelin, and M. Bleicher, *Phys. Rev. C* **78**, 044909 (2008).
  - [12] W. M. Yao *et al.* (Particle Data Group Collaboration), *J. Phys. G* **33**, 1 (2006).
  - [13] M. Bleicher and J. Aichelin, *Phys. Lett. B* **530**, 81 (2002).
  - [14] M. Bleicher, *Nucl. Phys. A* **715**, 85 (2003).
  - [15] M. Bleicher and H. Stoecker, *J. Phys. G* **30**, S111 (2004).
  - [16] S. Vogel and M. Bleicher, [arXiv:nucl-th/0505027](https://arxiv.org/abs/nucl-th/0505027).
  - [17] S. Vogel and M. Bleicher, *Phys. Rev. C* **74**, 014902 (2006).
  - [18] S. Vogel and M. Bleicher, *Phys. Rev. C* **78**, 064910 (2008).
  - [19] S. A. Bass *et al.*, *Prog. Part. Nucl. Phys.* **41**, 255 (1998).
  - [20] M. Bleicher *et al.*, *J. Phys. G* **25**, 1859 (1999).